

# Thorium-Normalized Airborne Radio- Spectrometric Data Technique , As A Guide To The Recognition Of Probable Subsurface Petroleum Accumulations, West Qasr Elfarafra Area, Western Desert , Egypt

Abd El Rahman R M. \* and El Hawary A.

Nuclear Materials Authority. , P.O. Box 530 El-Maadi, Cairo, Egypt.

Received: 9 Oct. 2022, Revised: 3 Nov. 2022, Accepted: 11 Dec. 2022

Published online: 1 Jan. 2023.

**Abstract:** Thourium normalization is a technique using surface and aerial gamma-ray spectral measurements in prospecting for petroleum in stratigraphic and structural traps. West Qasr El-farfra area, Central Western Desert, Egypt, was selected to apply this method on its recorded aerial gamma-ray spectrometric survey data, due to its distinct stratigraphic and structural setting as well as its situation with new discovered oil production fields in Egypt. Thorium normalization technique was first applied on well logging data by [1] who concluded that the results of thorium normalization agree with the results of well log analysis on the Lower Miocene (Rudeis) Formation in Belayim marine oil field in 82% of the cases studied. The three variables (eU, eTh, and K) registered for the whole study area, in the form of three contour maps, The DRAD arithmetic means plus two standard deviations for the data set were computed. Any single DRAD -value greater than this quantity should have a probability of 95% that it represents a valid anomaly and is not caused by random variations in the background values. The application of these criteria has led to the identification of five zones over the investigated area that is statistically valid. These might indicate a prospective possibility for feasible subsurface hydrocarbon accumulations and oil-bearing pay zones at west qasr elfarfra area.

**Keywords:** Farafara, Thorium Normalization.

## 1 Introduction

West Qasr Elfarafra Area is located in the Central Western Desert (Fig. 1), the study area is approximately 640 Km<sup>2</sup>. EL\_Farafa area is covered by thick sedimentary rocks range in age from Late Cretaceous (Campanian) to Eocene, and there are new discovered hydrocarbons accumulations. Airborne radiospectrometric survey was carried out by members of airborne geophysical project at Nuclear Materials Authority (NMA) in Egypt. The used spectrometer records 256 channels of spectral data in the range 0-3 MeV, and uses self-stabilizing to minimize spectral drift. A software program is used to monitor the photo-peak of gamma emitters usually potassium and thorium to adjust the gain of the detectors (auto-tuning).

## 2 Geological Descriptions

EL\_Farafa area is covered by various sedimentary rocks range in age from Late Cretaceous (Campanian) to Eocene. In addition, to some Quaternary sand dunes oriented in the NW-SE direction. According [4] Kurkur Formation (

Tarawan Formation ) Kurkur Formation comprises a calcareous facies deposit that caps El-Quss Abu Said plateau and the southeastern part of Farafra depression. It is deposited over the clayey deposits of Dakhla Formation with an erosional surface. It is composed of locally sandy to clayey fossiliferous reefal calcareous deposits, belonging to the Early Paleocene age [3,5] towards the north, this Formation passes laterally to a chalky facies characterizing. El-Farafa structural elements may represent the transitional stage between the typical stable and mobile shelf conditions. Faults, joints and folds indicate movements in the basement, but these are faintly distinguished on the surface due to the relatively thick sedimentary cover [2].

## 3 Methodologies

According to [6], Thorium normalization method was developed which uses surface and aerial gamma-ray spectral measurements in prospecting petroleum in stratigraphic and structural traps. Equivalent Uranium and potassium data for aerial subsurface gamma-ray spectral

\*Corresponding author e-mail: Mounir\_r79@yahoo.com



**Figure.1:** Location map of West Qasr Elfarfra Area, Central Western Desert, Egypt.

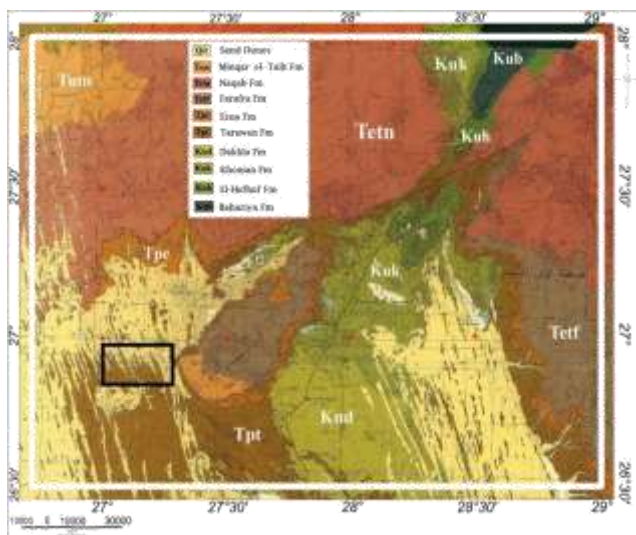


**Figure 2.** Geologic Map of Farafra Area, Central Western Desert, Egypt, (after Conoco, 1987)

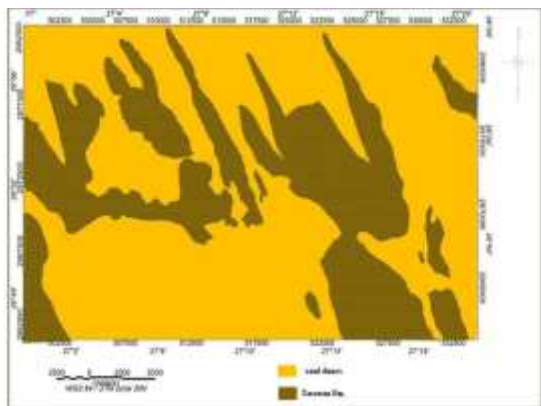


**Figure 3.** Geological map of west Qasr El Frafra area, central western desert, Egypt.

profiles were normalized to equivalent thorium data, using the procedures of [6]. Plots were made for the field of measured Ks versus eThs and eUs versus eThs values for all readings. The simplest effective Eqs; (1), (2) relating these variables were determined to be linear and pass

through the origin. The slopes of the lines were determined by the ratios of mean Ks to mean eThs, or mean eUs to mean eThs. The equations are:

$$K_i = (\text{mean } K_s / \text{mean } eThs) eThs \quad (1)$$

$$eU_i = (\text{mean } eU_s / \text{mean } eThs) eThs \quad (2)$$

Where  $K_i$  is the ideal equivalent thorium defined potassium value for the reading with a real equivalent thorium value of  $eThs$ , and  $eU_i$  is the ideal equivalent thorium defined equivalent uranium value for that reading. Using this approach, the equations were calculated directly from the data and quick field evaluations may be made without preparing the plots and resorting to curve fitting. Deviations of the real values from the calculated ideal values for each reading were

Obtained using equations of the form:

$$KD\% = (K_s - K_i) / eThs \quad (3)$$

$$eUD\% = (eU_s - eU_i) / eThs \quad (4)$$

where  $K_s$  and  $eU_s$  are the measured values at the reading stations, and  $KD\%$  and  $eUD\%$  are the relative deviations expressed as a fraction of the reading values. Experience has shown that  $KD\%$  yields small negative values and  $eUD\%$  yields smaller negative or sometimes positive values [6],  $KD\%$  and  $eUD\%$  variations can be combined as a single positive number,  $DRAD$ , which is the difference between both of them:

$$DRAD = eUD\% - KD\% \quad (5)$$

*Where positive DRAD values are favorable indications of petroleum accumulation*

## 4 Discussions and Interpretation of Data

### 4.1 Statistical Evaluation of Data

The characteristics and variations of  $DRAD$  values in areas not situated over identified oil or gas-producing fields may be estimated by examination of the profiles in those areas. The  $DRAD$  values in the study area range from -0.55 to 1.14. Most positive  $DRAD$  values are located in the northeastern part (Fig. 4). Lists ten selected profiles located over the study area which are not currently known to produce oil or gas, as well as arithmetic mean and standard deviation (Table 1). (Fig. 5) shows  $DRAD$  values that over the value of  $(\bar{x}+1S)$  and  $(\bar{x}+2S)$ . (Fig. 6) defines five zones of that may reflect zones of subsurface hydrocarbon accumulations. Deviation ( $S$ ) for each profile data set is treated as representing one population. A conservative estimate of background statistical parameters is based on the population. The mean  $DRAD$  arithmetic mean plus two standard deviations  $(\bar{x}+2S)$  reaches 0.751 (Table 1) for this data set (Table 1). Any single profile ( $\bar{x}$ ) value greater than this quantity has a probability of 95 % that it represents a valid anomaly is not caused by random variations in the background values [6-13]. The maximum  $DRAD$  mean

value were 0.165 in line No. 3 while the lowest mean were -0.224 in line No.10, lines 2,5,6, and 7 have a maximum DRAD value reached over 0.751 that may reflect zones of subsurface hydrocarbon accumulations

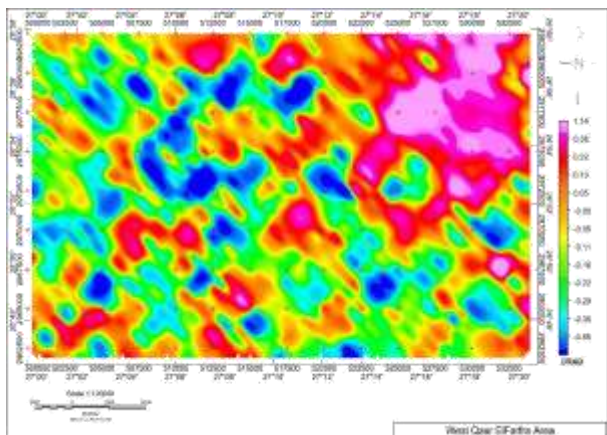


**Figure 4.** DRAD map west Qasr El-Farafra area, central western desert , Egypt.

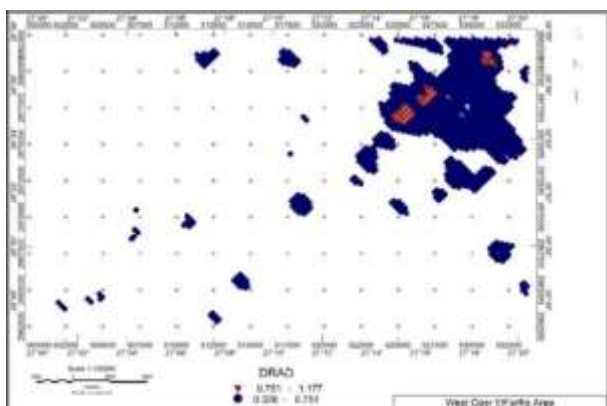


**Figure 5.** DRAD statistically anomalous zones , west Qasr El-Farafra area, central western desert , Egypt.

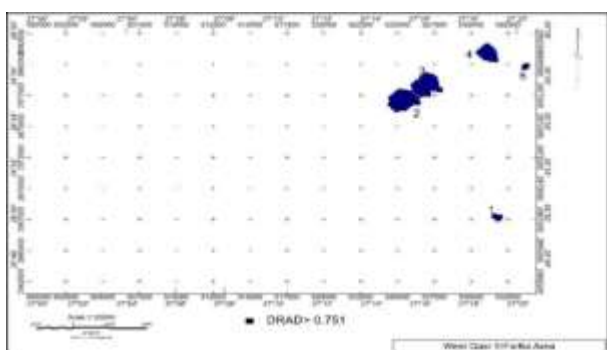


**Figure 6.** DRAD favorable zones( $\bar{x} + 2s$ )west Qasr El-Farafra area, central western desert , Egypt.

Comparative profiles of Ks,,eUs,, Ths, KD%, eUD%, and DRAD were plotted for 10 selected flight lines, to illustrate typical crossover. The following discussion is devoted only to three flight lines out of the 10, as examples.

Plots of the unprocessed and processed airborne radio-

spectrometric survey data with 200m station separation along each profile starting from north to south direction over the flight line (No. 2,6,and 7) are presented in Figs. 8,9, and 10.

These flight lines are located in the eastern part of the area. The unprocessed (measured or real) data for potassium (K) and equivalent thorium (eTh, ) line 2 Fig 8 A) show a well-defined relation at a distance ranging from station 0 to 70. Meanwhile, the unprocessed (measured or real) potassium (K,) data do not show any well-defined relation to those of eTh, and eU. The relatively higher measured values located in the northern part between stations 0 to 50 where the relatively lowest measured values located in the southern part. The plot of KD% in line No. 2 (Fig. 8 B) shows high (positive) eUD% and DRAD values between stations 0 to 50 then there were sharp negative values in DRAD, eUD% , and KD% values between stations 60 to 65 . The positive high DRAD value that reached 1.14) from stations 7 to 10 give favorable indication of possible hydrocarbon accumulations.

The plot of real eU, eTh, ,and K of line 6 (Fig 9A) shows that the highest eU, and eTh value located at station No. 20 reaches 7.5ppm ,and 16ppm respectively ,while the lowest measured station for the three radioactive elements was station No. 90. The plot of KD% in line No. 6 (Fig. 9B) shows a sharp negative between stations 22 to 25. This zone is accompanied by a positive eUD%, producing a crossover of eUD% and KD%, and positive DRAD values: Relatively high values of equivalent uranium in this zone may be the result of the gaseous uranium daughter, radon, leaking up and concentrating in an unmapped fault zone (s) and mainly composed of Quaternary Sediments. So, this zone reveals favorable indications of possible petroleum accumulations.

The plot of KD% in line No. 7 (Fig. 10B) shows high (positive) eUD% and DRAD values between stations 24 to 38. The positive high DRAD value that reached 1 from at station 28 give favorable indication of possible hydrocarbon accumulations.

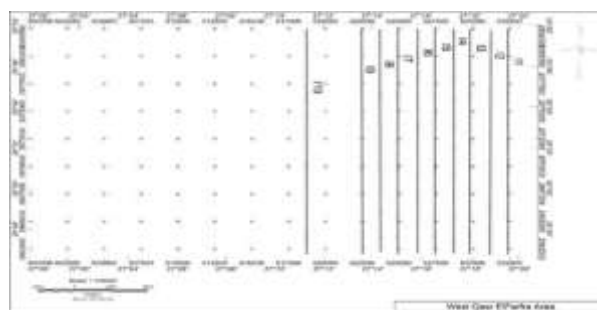


**Figure 7.** Ten selected profiles west El-Farafra area, Central Western Desert, Egypt.

**Table 1.** Statistical parameters computed for DRAD for the studied flight lines, West Qasr Elfarfra area central western desert Egypt.

Line No.	Min. value	Max. value	Mean. ( $\bar{x}$ )	Stand. Dev.	$\bar{X}+2s$	$\bar{x}+3s$
1	-0.500	0.600	0.066	0.308	0.683	0.991
2	-1.000	1.100	0.133	0.448	1.030	1.478
3	-0.600	0.700	0.165	0.329	0.822	1.151
4	-0.600	0.700	0.156	0.315	0.787	1.102
5	-0.500	0.800	0.145	0.320	0.785	1.105
6	-0.500	0.800	0.075	0.349	0.772	1.120
7	-0.600	0.900	0.062	0.362	0.785	1.147
8	-1.200	0.500	-0.035	0.371	0.707	1.078
9	-0.500	0.400	-0.073	0.232	0.391	0.623
10	-5.800	0.400	-0.224	0.913	1.603	2.516
Area	-12.64	1.14	-0.100	0.425	0.751	1.177

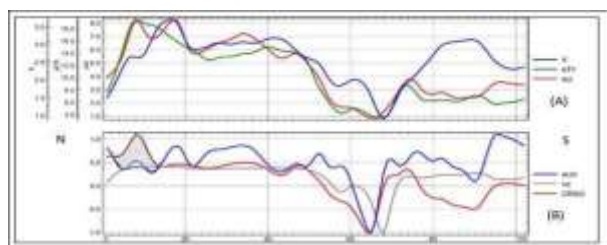


**Figure 8.** Selected line No. 2 profiles , the unprocessed ks ,eThs , and eUs data (A) , and the processed KD%,eUD% , and DRAD data (B) west qasr elfrafra area, Central Western Desert Egypt.

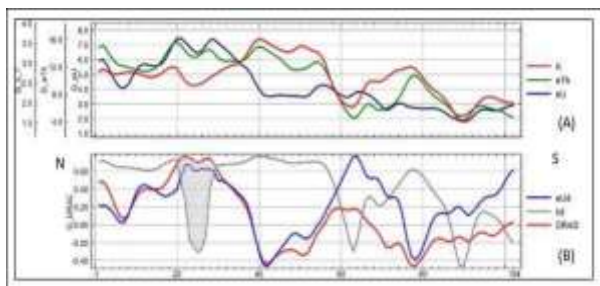


**Figure 9.** Selected line No. 6 profiles , the unprocessed ks ,eThs , and eUs data (A) , and the processed KD%,eUD% , and DRAD data (B) west qasr elfrafra area, Central Western Desert Egypt.

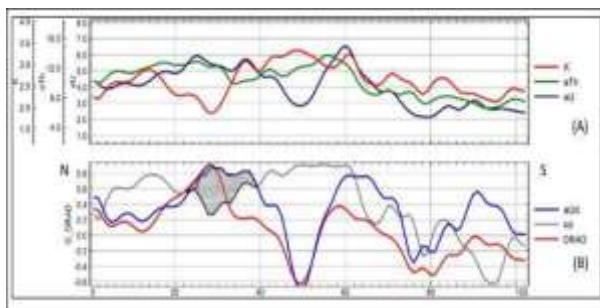


**Figure 10.** Selected line No. 7 profiles , the unprocessed ks ,eThs , and eUs data (A) , and the processed KD%,eUD% ,

and DRAD data (B) west qasr elfrafra area, Central Western Desert Egypt.

## 5 Conclusions

The three radioelements (eU,eTh, K) for west Qasr El-frafra area central western desert were mapped every 200m . comparative profiles of Ks, eUs, eThs , KD%,eUD% and DRAD were plotted for 10 flight lines to explain typical “crossover” anomalies over the area or zones which may indicate hydrocarbon accumulations . The characteristics and variations of DRAD in area not situated over identified oil or gas producing field may be estimated by examining the profiles in the area. The DRAD arithmetic mean plus two standard deviations reaches 0.75 for this area. There are five zones that have DRAD values greater than 0.75 which led to probability of 95% that is a valid anomaly and is not caused by random variations in the background values, and might indicate prospective hydrocarbon accumulations.

## References

- [1] Al-Alfey M. I Radioactivity and Reservoir Characteristics of Lower Miocene Rocks in Belayim Marine Oil Field, Gulf of Suez, Egypt, Ph.D, Zagazeg Univ.,177 P. 2008.
- [2] Barakat and Abdel Hamid Airphoto Interpretation of Some Structural Features in the Area South West of Aswan. Egypt. J. Geol.,**16(2)**, 247-254. 1073.
- [3] Hermina, M. Geology of the North-Western approaches of Kharga. Geol. Surv. Egypt, Pap., 44, 87p. 1976.
- [4] Hermina, M. The surrounding of Kharga, Dakhla and Farafra oases. In: R. Saïd (ed), The geology of Egypt, A.A. Balkema, Rotterdam., 259-293. 1990.
- [5] Issawi, B., Hassan, Y. and Saad, A. Geology of Abu Tartur plateau, Western Desert, Egypt. Egypt. Geol. Surv. Ann., **8**, 91 – 127. 1978.
- [6] Saunders, D. F., Burson, K. R., Branch, J. F., & Thompson, C. K. Relation of thorium- normalized surface and aerial radiometric data to subsurface petroleum accumulations. GEOPHYSICS., **58(10)**, 1417–1427. 1993.
- [7] A El-Taher Elemental analysis of two Egyptian phosphate rock mines by instrumental neutron activation analysis and atomic absorption spectrometry. Applied Radiation and Isotopes., **68(3)**, 511-515. 2010.
- [8] AE Abdel Gawad., MA Ali., MM Ghoneim and A. El-Taher., Natural radioactivity and mineral chemistry aspects of rare metal mineralisation associated with mylonite at Wadi Sikait, South Eastern Desert, Egypt International Journal of Environmental Analytical Chemistry., 1-18. 2021.
- [9] HM Zakaly, MA Uosif, H Madkour, M Tammam, S

- Issa, R Elsaman, Atef El-Taher Assessment of natural radionuclides and heavy metal concentrations in marine sediments in view of tourism activities in Hurghada city, northern Red Sea, Egypt. Penerbit Universiti Sains Malaysia., **3(30)**, 21-47. 2019.
- [10] A El-Taher, HA Madkour Environmental and radioecological studies on shallow marine sediments from harbour areas along the Red Sea coast of Egypt for identification of anthropogenic impacts. Isotopes in environmental and health studies., **50(1)**, 120-133. (2014).
- [11] AA Ibraheem, A El-Taher, MHM Alruwaili Assessment of natural radioactivity levels and radiation hazard indices for soil samples from Abha, Saudi Arabia. Results in Physics., **11**, 325-330. 2018.
- [12] KS Al-Mugren and A. El-Taher., Risk assessment of some radioactive and elemental content from cement and phosphate fertilizer consumer in Saudi Arabia. Journal of Environmental Science and Technology., **9(4)**, 323-328. 2016.
- [13] A. El-Taher and S Alashrah., Occurrence of  $^{222}\text{Rn}$  in irrigation water from Wadi Al-Rummah Qassim province, Saudi Arabia. AIP Conference Proceedings., **1674(1)**, 020007, 2015.